RJC

RASĀYAN *J. Chem.*
Vol. 13 | No. 2 |1000 - 1007| April - June | 2020
ISSN: 0974-1496 | e-ISSN: 0976-0083 | CODEN: RJCABP
http://www.rasayanjournal.com
http://www.rasayanjournal.co.in

# COMPARATIVE PHYSICAL STUDY OF EVANS BLUE BY $FE_3O_4$@CF-R COATED COMBINATION OF DECORATED GO AND $TIO_2$ MAGNETIC NANOCOMPOSITE

**Usha Jinendra[1], B. Lakshmi[2], Sachin Bhat[3,*] and B. Dinesh[4]**

[1,2,4]Department of Chemistry, REVA University, Bengaluru-560065, (Karnataka) India
[3]Department of ECE, Shri Madhwa Vadiraja Institute of Technology and Management, Bantakal, Udupi - 574115, (Karnataka) India
*E-mail: sachinbhat88@gmail.com

**ABSTRACT**

$Fe_3O_4$@coated@GO nanocomposite and $Fe_3O_4$@coated @TiO nanocomposite were arranged using utilizing the autoclave sonication strategy. The shell thickness of $Fe_3O_4$@ coated@ GO nanocomposite and $Fe_3O_4$@coated@TiO nanocomposite is successfully controlled within the extend of 44-54.47nm and 53.78-77.30 nm using shifting the response conditions. Particularly, Catechol bunches on the highest layer of nanospheres to play a critical part in chemistry to assist combined with graphene oxide (GO) to wrap the Fe3O4@ coated nanosphere. The gotten $Fe_3O_4$@ coated nanospheres and $Fe_3O_4$@ coated @GO nanocomposite can be utilized as the viable catalyst bolsters of little TiO nanoparticles combination. The prepared catalyst was proven for the diminishment of Evans blue color. The adsorption of the resultant proportion of $Fe_3O_4$@coated @GO and @TiO nanocomposites is affected by several variables like the nearness of isothermal, pH, contact time and temperature.

**Keywords:** Blue Dye, Magnetic Core-shell Nanocomposite, Physical Adsorption, Antibiological Studies



## INTRODUCTION

Historically, human population and industrial activities have led to an increase in water pollution. Synthetic chemical compounds and dyes form a new class of toxic waste in the water source. Their presence in water or biosphere is generally related to pollutants that have no control or whose effects are unknown and are suspected to affect the environment[1]. The presence of skyrocketing toxic and foreign matter in-ground/surface water resources used for drinking leads to a serious problem. Among the increasing pollutants, Evans Blue dye(direct blue-53dye or T-1824), a synthetic bis azo dye has retained a long history that is used directly on fibers and textiles. The Evans blue is classified as a toxic dye, which has chronic health effect, affecting the lung function, liver, urinary bladder, and intestine. Removal of such dyes is an important part of wastewater management before being released to environment[2]. The use of Graphite Oxide(GO) tea has shown good degradation properties due to improved charge separation, porous, stability in addition to its adsorption attributes[3]. It is long-familiar that 2D structural GO has a very-big specific surface area, 2D morphology and unique multi-functional surface chemical properties[4]. Earlier studies have established that GO contains ample oxygenated functionalities, which can be utilized to fix firm and stable interaction with other materials including polymers and metal oxides etc. Earlier studies have shown that GO has comprehensive oxygenated functionalities that can be used to remedy and stable contact with other materials, including polymers and metal oxides, etc. However, via their surface oxygen which contains functional groups or defects as nucleation sites, they adsorb and embed metal particles to form stable nanocomposites. However, it is infamous for a strong tendency to aggregate metal particles due to their van der Waals interaction or stacking, so graphene composites ' chemical fictionalization is an essential method for improving or solving the above problem[5]. Also, the metal/metal oxide composite materials supported by graphene are a kind of catalyst with great potential and have better catalytic performance compared to those ordinary catalysts which benefit from the formation of

*Rasayan J. Chem.*, 13(2), 1000-1007(2020)
**http://dx.doi.org/10.31788/RJC.2020.1325564**

stable metal particle-embedded graphene hybrids.[6-10] Due to this, we have prepared two nanocomposites and applied for the adsorptive degradation of Evans Blue Dye.[11]

## EXPERIMENTAL

### Material and Methods

Iron(II, III) oxide, Catechol($C_6H_6O_2$), titanium isopropoxide($TiO_2$), Formaldehyde ($CH_2O$), Anhydrous *Ammonia(*$NH_4OH$), Potassium permanganate ($KMnO_4$), *Tiny graphene oxide (GO), Tris buffer*, Formaldehyde($CH_2O$), Hydrogen peroxide($H_2O_2$), Sulphuric acid($H_2SO_4$) and Hydrochloric acid (HCl) are used without further purification. All the above-mentioned chemicals are AR grade with 99% purity. Ultra based water was used throughout the experiment. Synthesis and characterization of different compositions are given below.

### Synthesis of GO

Natural graphite powder was treated with a homogeneous acidic mixture of $H_2SO_4$ and o-$H_3PO_4$ with constant stirring in the ice bath for about 24hrs. $KMnO_4$ is gradually mixed and is heated to 50°C with continuous stirring. This is diluted in cold water with $H_2O_2$ at normal temperature and allowed to settle for 3hrs. The solution is washed with HCl until its pH value becomes neutral. The product is dried in an oven at 60°.

### Synthesis of $Fe_3O_4$ @ Catechol-Formaldehyde Resin(CF-R) Core-Shell Nanospheres

15mg of FeO.$Fe_3O_4$(Ferro ferric oxide) with 20ml of purocatechol and 10ml of $NH_4OH$ solution is mixed and is ultrasonicated for about 6hrs. $CH_2O$ is added to this and transferred to a steel autoclave heated at $160^0$c up to 2 hours[5]. The product generated after magnetic separation is washed in water and ethanol until the solution becomes neutral. It is dried in vacuum to get the core-shell nanospheres[6].

### Synthesis of $Fe_3O_4$@ CF-R-Decorated on GO Hybrid Nanocomposite (GO Nanocomposite)

15mgs of each GO powder and the above nanospheres are distributed in 75ml trisaminomethane solution under ultrasonication for 40 mins. Unadhered GO sheets are removed by washing and dried in a vacuum for 12h[7].

### Synthesis of $Fe_3O_4$@ CF-R-Decorated on $TiO_2$ Hybrid Nanocomposite($TiO_2$ Nanocomposite)

50mgs of $Fe_3O_4$@CF-R core-shell nanospheres are dispersed into 50ml absolute ethanol for 30mins. This black suspension is mixed with 3.7ml $TiO_2$ solution (0.1M) by ultra-sonication for 1h. The obtained solution is agitated at normal temperature for 24h without reducing agent. The product was collected through a magnet, unloaded $TiO_2$ was removed and dried in vacuum[7].

### Characterization of GO Nanocomposite and $TiO_2$ Nanocomposite

Magnetic $Fe_3O_4$@CF-R core-shell nanospheres are prepared by polycondensation of $C_6H_6O_2$ and $CH_2O$ catalyzed by $NH_4OH$ with magnetic $Fe_3O_4$ nanoparticles as the seeds under the autoclave condition. The outside part of magnetic $Fe_3O_4$- nanoparticles formed has an irregular surface. It can be seen that the coated nano-sphere shells onto the $Fe_3O_4$ nanoparticles, there is a strong different element interaction between catechol groups and Fe-O moieties. The Sphere structure leads to surface energy reduction on the coated nanospheres shell grown on the surface of $Fe_3O_4$- nanoparticles.

We studied the effect of other synthetic circumstances on the arrangement and shape of the above-said nanospheres[8]. The shell thickness is depending on the number of reactants of $CH_2O$ and $C_6H_6O_2$. GO nanocomposite has an irregular shape and $TiO_2$ nanocomposite is circular. Inquiry on the structural behavior of samples is accomplished through XRD method. Diffraction patterns of GO nanocomposite and $TiO_2$ nanocomposite are shown in Fig.-1.

SEM micrographs in Fig.-2 showed that nanocomposite of $TiO_2$ was synthesized with diameters 44-54nm and with the adding for the GO the diameter to be 55nm to 77.5nm. The morphology of the nanospheres did not change on attaching GO nanoparticles on them. However, the $TiO_2$ nanofibers agglomerated together on $Fe_3O_4$ compared with GO nanocomposite as shown which indicated that the catechol group on the nanospheres immobilized on the surface of GO lead to relatively weak interaction.[9]

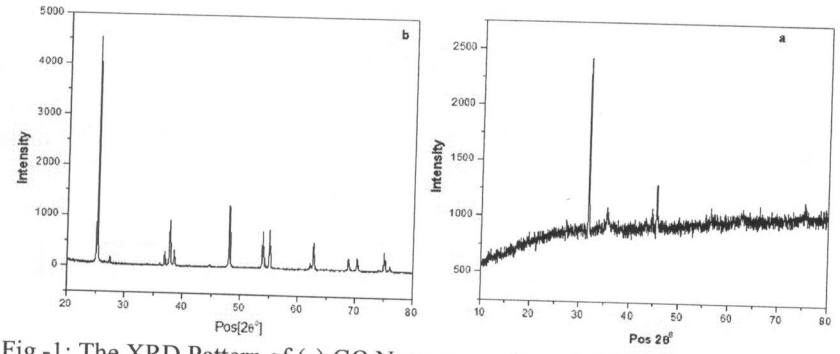


Fig.-1: The XRD Pattern of (a) GO Nanocomposite and (b) $TiO_2$ Nanocomposite

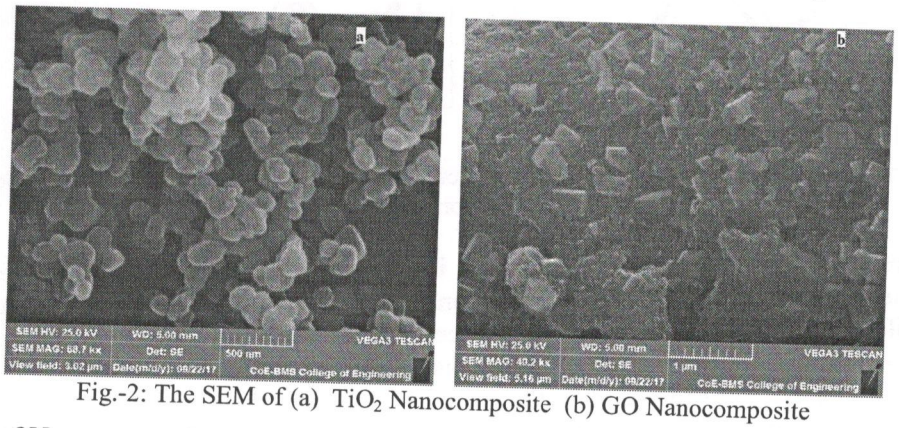


Fig.-2: The SEM of (a) $TiO_2$ Nanocomposite (b) GO Nanocomposite

**Performance of Nanocomposites for the Reduction of Evans Blue**

The fresh $NaBH_4$ solution (1 ml, 0.5 Mole) and Evans Blue solution (2 ml, 5 $mgL^{-1}$) are mixed and shaken up for 30 seconds. Catalysts GO nanocomposite(0.015 $mgL^{-1}$) and $TiO_2$ nanocomposite (0.017 $mgL^{-1}$) were gradually added to and the catalytic reaction is supervised. Collected nanocomposites were rinsed with water and ethanol for well clear water stability after separating them from the solution with a magnet.

## RESULTS AND DISCUSSION

**Selection and Optimization of Catalyst**

The catalytic activity of newly synthesized GO nanocomposite and $TiO_2$ nanocomposite were tested by deciding the reduction reaction of Evans Blue. Due to reaction kinetics, the blue solution will turn to colorless when 0.017 $mgL^{-1}$ of $TiO_2$ nanocomposite and 0.015 mg/L HCN1 are injected.

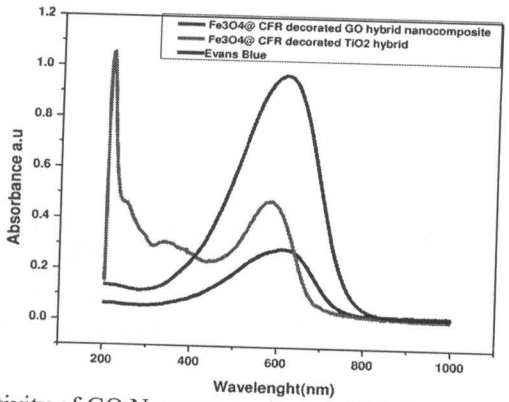


Fig.-3: Catalytic Activity of GO Nanocomposite and $TiO_2$ Nanocomposite on Evans Blue

Figure-3, shows the comparison of UV visible spectrophotometry for Evans blue catalyzed by GO nanocomposite and $TiO_2$ nanocomposite as catalysts respectively. It is visible from the graph that the

characteristic absorption band of Evan Blue at 622nm slowly drops post catalytic reaction. This is companioned by the rise of absorption peaks at 568 nm and at 624nm indicating the reduction of Evans Blue based on the color change from blue to colorless. Absorbance as a function of reaction time (t) for the catalysts was studied. As observed in Figures-4a and 4b, the reaction rate of GO nanocomposite is much faster than the $TiO_2$ nanocomposite.

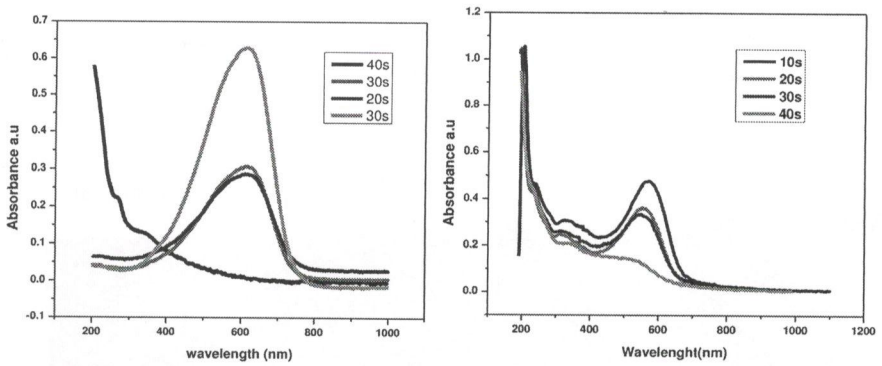


Fig.-4: Comparison of Absorbance and Wavelength as a Function of Reaction Time (t) for (a) GO Nanocomposite (b) $TiO_2$ Nanocomposite

The high catalytic activity should be attributed to the interaction of nano-catalysts with the substrate Evans Blue and is reduced due to the accommodation of dye particles in the vacant portions. The absorption rate will be slowed down in the coming stages due to this. The removal curves were single, smooth and continuous, indicating single layer coverage of dye on the surface of the adsorbent. The Evans Blue molecules have a +ve charge, while the coated nanospheres shell or GO layers on the surface of catalysts possess a -ve charge across the pH values.[11]

Therefore, the electrostatic attraction among the Evans Blue and coated nanospheres result in the rapid improvement of the Substrate to the surfaces of the catalysts at both ends, creating a locally concentrated layer. And the reduction reaction occurs through the electron transfer systems which generate an intermediate redox potential on the surface of TiO2 NPs between the donor and the acceptor[11]. Results in fig.5 have shown that the absorption capacity has improved with the higher concentration of dye and pH. Also, it is observed that an increase in dye concentration leads to an increase in equilibrium time. This is mainly due to the existence concentration gradient which raises the driving force and absorption capacity by transferring the molecules in between liquid solution and solid catalyst[12].

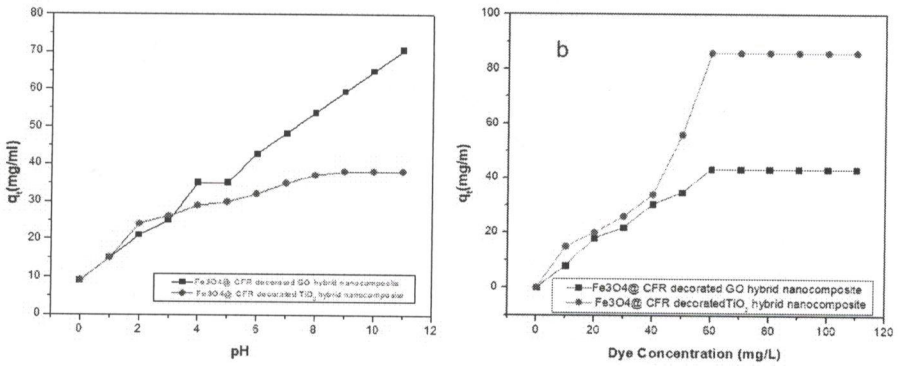


Fig.-5. Factors Affecting on Adsorption Capacity of Evans Blue (a) pH, (b) Initial Dyes Concentration

**Adsorption Isotherms**

To know the relation between adsorbate concentration on the solution and adsorbent surface, we have applied Langmuir(L), Freundlich(F) and Tempkin(T) isotherms[14] as shown in Fig.-6 and Table-1. It can be observed that the correlation coefficient($R^2$) in F & L isotherms are high. However, the adsorption capacity of L(0.9992) is greater than F(0.986). On the heterogeneous surface of the adsorbent mixed

oxide $Fe_3O_4$@CF-R decorated GO (Spheres and sheets), regions can occur with the $-OH$ and $-OH^{2+}$ groups based on the pH of a solution. Also, the formation of a multi-layer of dye through the adsorption process has taken place[13].

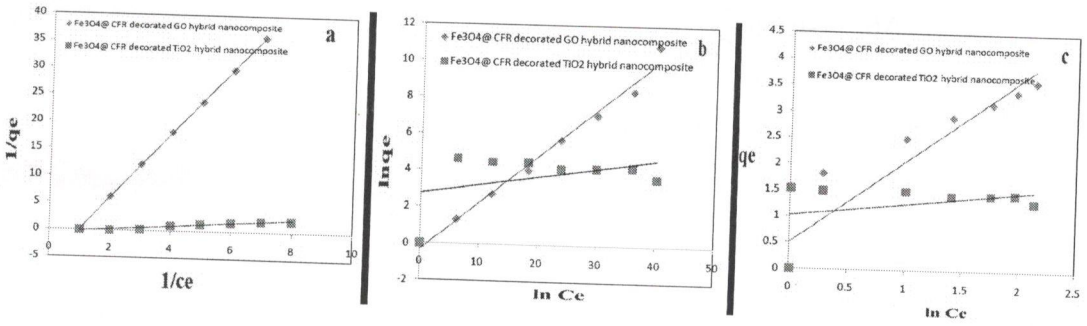


Fig.-6: a, b and c show the Langmuir, Freundlich and Tempkin Isotherms of Evans Blue

Table.-1: Correlation Coefficient for the Adsorption of Evan Blue

| Isothermal | $R^2$ | $R^2$ |
|---|---|---|
| | GO nanocomposite | $TiO_2$ nanocomposite |
| Langmuir Isothermal | 0.999 | 0.959 |
| Freundlich Isothermal | 0.986 | 0.199 |
| Tempkin Isothermal | 0.891 | 0.151 |

**Kinetics Study**

Two well known kinetic models are investigated to get the best-fitted model for the experimental data obtained[18]. Figure-7(a) and (b) show the pseudo 1st and 2nd order of Evans Blue. The compatibility of the chemical adsorption process with pseudo 2nd order duo to $R^2$=0.936 can be observed in Table-2.

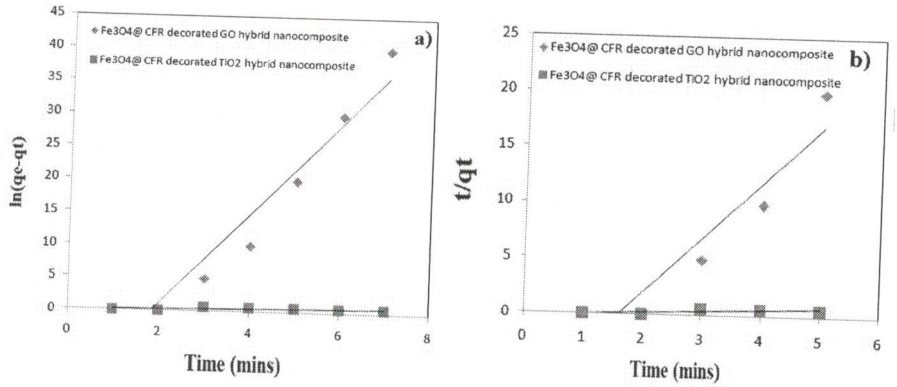


Fig.-7: Pseudo (a)First Order (b) Second Order

Table.-2: Kinetic Parameter of Evan Blue

| Kinectic Study | GO Nanocomposite | $TiO_2$ Nanocomposite |
|---|---|---|
| pseudo 1st order | $R^2$=0.936 | $R^2$= 0.625 |
| pseudo 2nd order | $R^2$=0.85 | $R^2$= 0.75 |

**Effect of Temperature**

Temperature plays an important role in the degradation of dye on catalysts. Figure-6 shows the increase of adsorption capacity of dye(50μ mol/L) with the increased temperature. This suggests that the process is endothermic. It is enhanced by an increase in temperature due to the diffusion rate of the adsorbent (dye molecules) across the external boundary layer and increased in the internal pores of the catalyst (adsorbent), thus increasing adsorption[12]. Thermodynamic parameters of the adsorption are given by Van't Hoff equation from eqs.-1 to 3.

$$\ln K^0 = \frac{\Delta S^0}{1R} - \frac{\Delta H^0}{rRT} \quad (1)$$

$$K^0 = \frac{q_e}{C_e} \quad (2)$$

$$\Delta G^0 = -RT \ln \frac{q_e}{C_e} \quad (3)$$

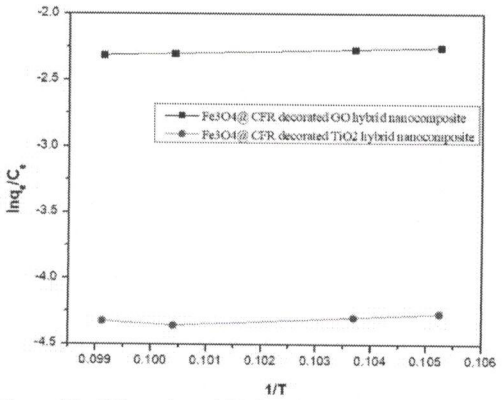


Fig.-8: Plot of ln K° against 1/T for the Adsorption of Evans Blue

Where, R is gas constant, ΔS and ΔH are entropy and enthalpy changes, ΔG is Gibbs free energy change. A straight line is plotted between ln K° and 1/T as shown in Fig.-8. Table-3 gives the value of thermodynamic parameters. Due to the +ve and higher value of ΔH, it can be seen that the process in chemisorptions and endothermic. +ve value of ΔS points to the high ordering of reaction during adsorption. -ve value of ΔG suggests to spontaneous process and the value increased at the higher temperature which refers to the adsorption process is preferably at elevated temperature.

Table.-3: Thermodynamic Parameters of the Adsorption of Evans Blue

| Temp | GO Nanocomposite | | | | $TiO_2$ Nanocomposite | | | |
|---|---|---|---|---|---|---|---|---|
| | $\Delta H^o$ | $\Delta S^o$ | $\Delta G^o$ | $R_2$ | $\Delta H^o$ | $\Delta S^o$ | $\Delta G^o$ | $R_2$ |
| +K | (kJ/mol ) | (J/mol.K) | (kJ/mol) | | (kJ/mol. ) | (J/mol.K) | (kJ/mol) | |
| 225 | 183.6 | 1.641 | -4.3241 | 0.85 | 350 | 2.64 | -2.31153 | 1 |
| 228 | | | -4.3572 | | | | -2.29858 | |
| 236 | | | -4.2962 | | | | -2.2664 | |
| 240 | | | -4.2689 | | | | -2.25147 | |

**Antibacterial Activity Studies**

**Antibacterial Screening**

The antibacterial activity of the above nanoparticles was tested against Gram positive bacteria namely *Staphylococcus aureus,* and Gram-negative bacteria namely *Escherichia coli* and *Salmonella typhi*by agar well diffusion method. Twenty-four old Muller-Hinton broth cultures of test bacteria were swabbed on sterile Muller-Hinton agar plates using sterile cotton swab followed by punching wells of 6 mm with the help of sterile corkborer. The standard drug (Chloramphenicol, 100 µg/mL of sterile distilled water), three different concentrations (100, 50 and 25 µg $mL^{-1}$ in 10% distilled water) of GO nanocomposite and $TiO_2$ nanocomposite and control (10% distilled water) were added to respectively labeled wells. These plates were allowed to stand for 30 min. and incubated at 32°C for 24 h in an upright position and the zone of inhibition was recorded. During this period, the test solution diffused zones of inhibition were recorded using Vernier callipers.

**Antifungal Screening**

The antifungal activity of the above nanocomposites evaluated against *Aspergillus niger* and *Penicillium chrysogenum* fungus, using the sabouroud dextrose agar diffusion method. Wells were made with a sterile

corkborer (6 mm diameter). The standard drug (Fluconazole, 100 µg/mL of sterile distilled water) and control (10% distilled water) were added to respectively labeled wells. To these wells, 140µL from each (100, 50, 25, 12.5, 6.25, 3.125 and 1.56 µg/mL in 10% distilled water) of the test stock solution compounds were added and the plates were allowed to cool for an hour to facilitate the diffusion. The plates were then incubated at 32°C for 52h. At the end of the incubation period, the diameter of the zone of inhibition around the wells was measured using Vernier scale. Both the activities with minimum inhibition concentration are recorded in table 4 and table 5.

Table.-4: Antimicrobial Activity of the Compounds (Zone of Inhibition in mm, mean ±SD at 100µg/mL)

| Compounds (100µg/mL) | Bacteria in mm | | | Fungi | |
|---|---|---|---|---|---|
| | *S.aureus* | *E.coli* | *S.typhi* | *A.niger* | *P.crysogenum* |
| 1 | 15.0 ± 0.1 | 13.3 ± 0.2 | 12.2± 0.1 | 5.0 ± 0.1 | 7.1 ± 0.1 |
| 2 | 14.0 ± 0.0 | 12.0 ±0.1 | 10.3 ±0.1 | 7.3 ± 0.2 | 8.4 ± 0.2 |
| 3 | 13.2 ± 0.1 | 10.5 ± 0.5 | 09.4 ± 0.2 | 6.9 ± 0.1 | 9.0 ± 0.3 |
| 4 | 15.4 ± 0.1 | 16.0 ± 0.2 | 13.8 ± 0.1 | 6.0 ± 0.1 | 6.2 ± 0.1 |
| 5 | 10.0 ± 0.0 | 13.2 ± 0.2 | 11.6 ± 0.2 | 8.2 ± 0.2 | 5.3 ± 0.1 |
| 6 | 12.6 ± 0.2 | 11.7 ± 0.3 | 08.7 ± 0.4 | 9.2 ± 0.2 | 8.7 ± 0.1 |
| GO nanocomposite | 22.0 ± 0.2 | 21.0 ± 0.1 | 25.0 ± 0.10 | | |
| $TiO_2$ nanocomposite | | | | 18.0 ± 0.20 | 20.0 ± 0.10 |

[#]*Chloramphenicol,* [*]*Fluconazole,* (n=3)

Table.-5: Minimum Inhibition Concentration (MIC)

| Compound | MIC of the Compounds (µg/mL) | | | | |
|---|---|---|---|---|---|
| | *S.aureus* | *E. coil* | *S.typlei* | *A.Niger* | *P.Crysogenum* |
| 1 | 50 | 25 | 25 | 100 | 100 |
| 2 | 50 | 50 | 50 | 100 | 100 |
| 3 | 25 | 25 | 50 | 50 | 100 |
| GO nanocomposite | 1.56 | 1.56 | 1.56 | - | - |
| $TiO_2$ nanocomposite | - | - | - | 3.125 | 3.125 |

## CONCLUSION

In short, magnetic core-shell nanospheres covered in stable coatings have for the first moment been manufactured effectively with a convenient and effective path. The as-prepared Fe3O4@coated thermal nanospheres@TiONPs and Fe3O4@coated nanospheres@GO@TiONPs have shown an extremely quick catalyst property for the response of coloring degradation. The new magnetic coated nanospheres based on hybrid nanospheres can thus discover more future commercial applications for heterogeneous catalysis as a stable support for elevated active metal nanoparticles.

## REFERENCES

1. T.Parandhaman, N.Pentela, B.Ramalingam, D.Samanta, S.K. Das, *ACS Sustainable Chemistry & Engineering*, **5(1)**, 489(2017), **DOI:**10.1021/acssuschemeng.6b01862.
2. X.Fei, W.Kong, X.Chen, X.Jiang, Z.Shao, J.Y. Lee, *ACS Catalysis*, **7(4)**, 2412(2017), **DOI:**10.1021/acscatal.6b03185
3. S.Navalon, A.Dhakshinamoorthy, M.Alvaro, H.Garcia, *Coordination Chemistry Reviews*, **312**, 99(2016), **DOI:**10.1016/j.ccr.2015.12.005
4. V.NirmalaDevi, M.Makeswari, *Rasayan Journal Chemistry*, **11(1)**, 219(2018), **DOI:**10.7324/RJC.2018.1111986
5. J. Liu, X. Huo, T. Li, Z. Yang, P. Xi, Z. Wang, B. Wang, *Chemistry-A European Journal*, **20(36)**, 11549(2014), **DOI:**10.1002/chem.201402545
6. G.M. Scheuermann, L.Rumi, P.Steurer, W.Bannwarth, R.Muulhaupt, *Journal of the American Chemical Society*, **131(23)**, 8262(2009), **DOI:**10.1021/ja901105a

7. Y.Cheng, Y.Fan, Y.Pei, M.Qiao, *Catalysis Science and Technology*, **5(8)**, 3903(2015), **DOI:** 10.1039/C5CY00630A
8. Y.Xie, B.Yan, H.Xu, J.Chen, Q.Liu, Y.Deng, H.Zeng, *ACS Applied Materials and Interfaces*, **6(11)**, 8845(2014), **DOI:**10.1021/am501632f.
9. S.Yamamoto, H.Kinoshita, H.Hashimoto, Y.Nishina, *Nanoscale*, **6**, 6501(2014), **DOI:**10.1039/c4nr00715h.
10. Y.Yang, C.E. Castano, B.F. Gupton, A.C. Reberb, S.N. Khanna, *Nanoscale*, **8**, 47(2016), **DOI:**10.1039/C6NR06793J.
11. J. Zhou, B. Duan, Z. Fang, J. Song, C. Wang, P. B. Messersmith, H. Duan, *Advanced Materials*, **26(5)**, 701(2014), **DOI:**10.1002/adma.201303032.
12. Y.K. Long, Q.Cao, *Powder Technology*, **310**, 24(2017), **DOI:**10.1016/j.powtec.2017.01.013
13. T.Vats, R.Gogoi, P.Gaur, A.Sharma, S.Ghosh, P.F. Siril, *Sustainable Chemistry and Engineering*, **5(9)**, 7632(2017), **DOI:**10.1021/acssuschemeng.7b00960.
14. N.Hoda, E.Bayram, E.Ayranci, *Journal of Environmental & Analytical Toxicology* **137**, 1 (2006), **DOI:**10.4172/2161-0525.1000264

[RJC-5564/2019]